

Density functional theory for dense nematics with steric interactions

Xiaoyu Zheng¹ Jamie M. Taylor² Peter Palffy-Muhoray³
 Epifanio G. Virga^{2*}

¹Department of Mathematical Sciences, Kent State University, OH, USA

²Mathematical Institute, University of Oxford, Oxford, UK

³Liquid Crystal Institute, Kent State University, OH, USA

March 3, 2017

Abstract

The celebrated work of Onsager [1] on hard particle systems, based on the truncated second order virial expansion, is valid at relatively low volume fractions and for large aspect ratio particles. While it predicts the isotropic-nematic phase transition, it fails to provide a realistic equation of state in that the pressure remains finite for arbitrarily high densities. In this work, we derive a mean field density functional form of the Helmholtz free energy for nematics with hard core repulsion. In addition to predicting the isotropic-nematic transition, the model provides a more realistic equation of state. The energy landscape is much richer, and the orientational probability distribution function in the nematic phase possesses a unique feature—it vanishes on a nonzero measure set in orientational space.

1 Introduction

An ensemble of non-spherical particles, interacting via hard core interactions, exhibits a first order isotropic-nematic phase transition as the number density increases, followed by a nematic-solid transition [2]. In his celebrated theoretical work [1], Onsager successfully predicted the isotropic-nematic transition. Using the canonical ensemble, he expressed the free energy in terms of the orientational probability density function $f(\hat{\mathbf{I}})$, where $\hat{\mathbf{I}}$ is a unit vector along the symmetry axis of a particle. Truncating the virial expansion after the second term, in the low volume fraction limit, the free energy per particle is of the form

$$F = kT \int_{\mathbb{S}^2} f(\hat{\mathbf{I}}) \left(\ln f(\hat{\mathbf{I}}) + \frac{1}{2} \rho_0 \int_{\mathbb{S}^2} f(\hat{\mathbf{I}}') V_{ex}(\hat{\mathbf{I}}, \hat{\mathbf{I}}') d\hat{\mathbf{I}}' \right) d\hat{\mathbf{I}}, \quad (1)$$

where k is Boltzmann's constant, T is the temperature and ρ_0 is number density.¹ In addition to the isotropic-nematic transition, the model describes phase separation and the coexistence of nematic and isotropic phases. In spite of its many successes, the theory has a major limitation: it cannot correctly describe the behavior near the dense packing limit. It does not give a reasonable equation of state; the pressure remains finite at arbitrarily high number density.

*Permanent address: Dipartimento di Matematica, Università di Pavia, Pavia, Italy

¹ A justification of Eq. (1) can also be given in terms of a reduced cluster expansion, based only on Penrose's spanning trees, which provides an explanation for the success of Onsager's theory better than the omission of all terms in the virial expansion but the first [3].

In this paper, the density functional theory of aspherical hard particles is revisited. We are particularly interested in the phase behavior of hard ellipsoids at high densities, and near densest packing limit. Our model is essential and approximate; the evaluation of the partition function at high densities, even for hard spheres, has eluded researchers to date in spite of considerable effort. Nonetheless, we feel it may reasonably capture a salient aspect of the problem: the depletion of available phase space as the density is increased.

Our key result is the striking fact that at densities above the isotropic-nematic transition, the orientational distribution function which minimizes the free energy has a compact support over orientation space. We also find that the nematic phase is more orientationally ordered than in Onsager theory at the same density. More importantly, but not surprisingly, our simple model gives a reasonable equation of state; that is, the pressure diverges at the dense packing limit.

The goal of the paper is to provide an approximate but realistic description of dense orientationally ordered hard particle systems; currently available descriptions are either low density approximations [4, 5], or they rely on somewhat *ad hoc* Carnahan-Starling type corrections to the free energy at high densities [6, 7]. We are interested in gaining insights into what happens at high densities when the system runs out of available phase space.

In section II, we write down the free energy of systems of hard ellipsoids with arbitrary number density, derive and solve the Euler-Lagrange equation for the probability density function, and derive the equation of state. In section III, we assume uniaxial nematic order, and present some numerical results. In section IV, we explore the possibility of biaxial equilibrium phases.

2 Model

We consider a one-component system consisting of hard ellipsoids. For simplicity, we omit attractive interactions. The configurational Helmholtz free energy of a system of N particles, within an additive constant, is

$$F = -kT \ln \frac{1}{N!} \int_{\Omega^N} e^{-\frac{1}{kT} \sum_{1 \leq i < j \leq N} U_{ij}^R} d\mathbf{q}_1 \cdots d\mathbf{q}_N, \quad (2)$$

where \mathbf{q}_i is the generalized (orientational and positional) coordinate of the i^{th} particle, and $U_{ij}^R = U^R(\mathbf{q}_i, \mathbf{q}_j)$ is the repulsive interaction energy between particles i and j , the sum is over all pairs of particles. Explicitly, the interaction potential is

$$U^R(\mathbf{q}_i, \mathbf{q}_j) = \begin{cases} \infty, & \text{if particles interpenetrate,} \\ 0, & \text{otherwise.} \end{cases} \quad (3)$$

We write

$$G_N = \int_{\Omega^N} e^{-\frac{1}{kT} \sum_{1 \leq i < j \leq N} U_{ij}^R} d\mathbf{q}_1 \cdots d\mathbf{q}_N, \quad (4)$$

where quantity G_N can be thought of as the number of states available to N distinguishable particles. We consider adding one particle to the system. Then

$$G_{N+1} = \int_{\Omega^N} e^{-\frac{1}{kT} \sum_{1 \leq i < j \leq N} U_{ij}^R} \left(\int_{\Omega} e^{-\frac{1}{kT} \sum_{i=1}^N U_{i(N+1)}^R} d\mathbf{q}_{N+1} \right) d\mathbf{q}_1 \cdots d\mathbf{q}_N, \quad (5)$$

and, since the probability density function of a given configuration is

$$P(\mathbf{q}_1, \cdots, \mathbf{q}_N) = \frac{e^{-\frac{1}{kT} \sum_{1 \leq i < j \leq N} U_{ij}^R}}{G_N}, \quad (6)$$

we have

$$\begin{aligned} G_{N+1} &= G_N \int_{\Omega^N} P(\mathbf{q}_1, \dots, \mathbf{q}_N) \left(\int_{\Omega} e^{-\frac{1}{kT} \sum_{i=1}^N U_{i(N+1)}^R} d\mathbf{q}_{N+1} \right) d\mathbf{q}_1 \cdots d\mathbf{q}_N \\ &= G_N \left\langle \int_{\Omega} e^{-\frac{1}{kT} \sum_{i=1}^N U_{i(N+1)}^R} d\mathbf{q}_{N+1} \right\rangle, \end{aligned} \quad (7)$$

where the averages is computed relative to P . Since all particles are equivalent, we write

$$G_N = \left\langle \int_{\Omega} e^{-\frac{1}{kT} \sum_{i=2}^N U_{1i}^R} d\mathbf{q}_1 \right\rangle^N, \quad (8)$$

where the integral represents the average free volume per particle in an ensemble of N particles. We can equivalently write this as

$$G_N = \left\langle \int_{\Omega} 1 - (1 - e^{-\frac{1}{kT} \sum_{i=2}^N U_{1i}^R}) d\mathbf{q}_1 \right\rangle^N \quad (9)$$

$$= \left(\int_{\Omega} (1 - W_1(\mathbf{q}_1)) d\mathbf{q}_1 \right)^N, \quad (10)$$

where

$$W(\mathbf{q}_1) = \left\langle 1 - e^{-\frac{1}{kT} \sum_{i=2}^N U_{1i}^R} \right\rangle \quad (11)$$

is the average excluded volume fraction. We estimate this quantity as

$$W(\mathbf{q}_1) = \int_{\Omega} \rho(\mathbf{q}_2) (1 - e^{-\frac{U^R(\mathbf{q}_1, \mathbf{q}_2)}{kT}}) d\mathbf{q}_2, \quad (12)$$

where $\rho(\mathbf{q}_2)$ is the number density of particles with generalized coordinate \mathbf{q}_2 .

The free energy then becomes

$$F = -kT \ln \frac{1}{N!} \left(\int_{\Omega} (1 - W(\mathbf{q}_1)) d\mathbf{q}_1 \right)^N. \quad (13)$$

The integral in Eq. (13) can be regarded as the fraction of the total volume available to particle 1, or the free volume fraction.

To obtain the density functional form of the free energy, we assume that the density $\rho(\mathbf{q}_i)$ is a slowly varying function of \mathbf{q}_i . We consider an element Ω_i of phase space, containing N_i particles and having volume $d\mathbf{q}_i$, sufficiently small so that $\rho(\mathbf{q}_i)$ in element i is nearly constant. The free energy F_i of region Ω_i is of the form of Eq. (13); that is, by Stirling's approximation,²

$$F_i = -kT \ln \left(\frac{1}{N_i} \int_{\Omega_i} 1 - W(\mathbf{q}_i) d\mathbf{q}_i \right)^{N_i}, \quad (14)$$

and since $\rho(\mathbf{q}_i)$ is nearly constant, we have that $N_i = \rho(\mathbf{q}_i) d\mathbf{q}_i$, and

$$F_i = -kT \ln \left(\frac{1}{\rho(\mathbf{q}_i)} (1 - W(\mathbf{q}_i)) \right)^{\rho(\mathbf{q}_i) d\mathbf{q}_i}. \quad (15)$$

² To be precise, the term $-kTN_i$ has been omitted on the right-hand side of Eq. (14). Its inclusion would only add a term proportional to the total number of particles to the right hand side of Eq. (17).

Then, since the free energy is additive, we can write for the entire system

$$F = -kT \ln \prod_i \left(\frac{1}{\rho(\mathbf{q}_i)} (1 - W(\mathbf{q}_i)) \right)^{\rho(\mathbf{q}_i) d\mathbf{q}_i}, \quad (16)$$

or

$$F = kT \int_{\Omega} \rho(\mathbf{q}) \ln \rho(\mathbf{q}) d\mathbf{q} - kT \int_{\Omega} \rho(\mathbf{q}) \ln(1 - W(\mathbf{q})) d\mathbf{q}, \quad (17)$$

which is the standard density functional form. Explicitly, this is

$$F = kT \int_{\Omega} \rho(\mathbf{q}_1) \ln \rho(\mathbf{q}_1) d\mathbf{q}_1 - kT \int_{\Omega} \rho(\mathbf{q}_1) \ln \left(1 - \int_{\Omega} \rho(\mathbf{q}_2) (1 - e^{-\frac{U^R(\mathbf{q}_1, \mathbf{q}_2)}{kT}}) d\mathbf{q}_2 \right) d\mathbf{q}_1. \quad (18)$$

For our problem, it is convenient to write the generalized coordinates in terms of position and orientation, then

$$F = kT \int_{\mathbb{S}^2} \int_{\mathcal{B}} \rho(\mathbf{r}_1, \hat{\mathbf{l}}_1) \ln \rho(\mathbf{r}_1, \hat{\mathbf{l}}_1) d^3 \mathbf{r}_1 d^2 \hat{\mathbf{l}}_1 - kT \int_{\mathbb{S}^2} \int_{\mathcal{B}} \rho(\mathbf{r}_1, \hat{\mathbf{l}}_1) \ln \left(1 - \int_{\mathbb{S}^2} \int_{\mathcal{B}} \rho(\mathbf{r}_2, \hat{\mathbf{l}}_2) (1 - e^{-\frac{U^R(\mathbf{r}_1, \hat{\mathbf{l}}_1, \mathbf{r}_2, \hat{\mathbf{l}}_2)}{kT}}) d^3 \mathbf{r}_2 d^2 \hat{\mathbf{l}}_2 \right) d^3 \mathbf{r}_1 d^2 \hat{\mathbf{l}}_1, \quad (19)$$

where $\rho(\mathbf{r}, \hat{\mathbf{l}})$ is the number density of particles with center of mass at position \mathbf{r} , and orientation of symmetry axis along $\hat{\mathbf{l}}$. \mathbb{S}^2 denotes orientation space, the surface of unit sphere. \mathcal{B} denotes position space, occupied by particles. In a homogeneous system, the density is independent of \mathbf{r} , so we write

$$\rho(\mathbf{r}, \hat{\mathbf{l}}) = \rho_0 f(\hat{\mathbf{l}}), \quad (20)$$

where ρ_0 now is simply the number density of particles, and $f(\hat{\mathbf{l}})$ is the single particle orientational distribution function satisfying

$$\int_{\mathbb{S}^2} f(\hat{\mathbf{l}}) d^2 \hat{\mathbf{l}} = 1. \quad (21)$$

Integrating over \mathbf{r}_2 gives

$$\int_{\mathbb{S}^2} \int_{\mathcal{B}} \rho_0 f(\hat{\mathbf{l}}_2) (1 - e^{-\frac{U^R(\mathbf{r}_1, \hat{\mathbf{l}}_1, \mathbf{r}_2, \hat{\mathbf{l}}_2)}{kT}}) d^3 \mathbf{r}_2 d^2 \hat{\mathbf{l}}_2 = \rho_0 \int_{\mathbb{S}^2} f(\hat{\mathbf{l}}_2) V_{exc}(\hat{\mathbf{l}}_1, \hat{\mathbf{l}}_2) d^2 \hat{\mathbf{l}}_2, \quad (22)$$

where

$$V_{exc}(\hat{\mathbf{l}}_1, \hat{\mathbf{l}}_2) = \int_{\mathcal{B}} (1 - e^{-\frac{U^R(\mathbf{r}_1, \hat{\mathbf{l}}_1, \mathbf{r}_2, \hat{\mathbf{l}}_2)}{kT}}) d^3 \mathbf{r}, \quad (23)$$

is the excluded volume of two particles, which depends only on the relative orientation of the two particles with respect to one another. Under such assumptions, the free energy becomes

$$F = kT \rho_0 V \left(\ln \rho_0 + \int_{\mathbb{S}^2} f(\hat{\mathbf{l}}_1) \ln f(\hat{\mathbf{l}}_1) d^2 \hat{\mathbf{l}}_1 - \int_{\mathbb{S}^2} f(\hat{\mathbf{l}}_1) \ln \left(1 - \rho_0 \int_{\mathbb{S}^2} f(\hat{\mathbf{l}}_2) V_{exc}(\hat{\mathbf{l}}_1, \hat{\mathbf{l}}_2) d^2 \hat{\mathbf{l}}_2 \right) d^2 \hat{\mathbf{l}}_1 \right). \quad (24)$$

If ρ_0 is small, one can expand the logarithm and recover the theory of Onsager as well as that of Doi and Edwards [8], apart from an inessential numerical factor.³ We note that the expansion is only valid when

$$\rho_0 \int_{\mathbb{S}^2} f(\hat{\mathbf{l}}_2) V_{exc}(\hat{\mathbf{l}}_1, \hat{\mathbf{l}}_2) d^2 \hat{\mathbf{l}}_2 < 1. \quad (25)$$

³For a gas of hard spheres, van Kampen [9] had already proposed a free energy that features the logarithm of the free volume. However, his derivation, which admittedly follows closely unpublished work of L.S. Ornstein (1908), is *ad hoc* and finds implicit inspiration in the exact treatment of one dimensional Tonks' gas [10].

In general, the argument of logarithm must be positive. The equilibrium orientational distribution $f(\hat{\mathbf{I}})$ is a function of ρ_0 , and is not known *a priori*. Intuitively, one would expect particles to align more and more as the number density is increased, indicating a decrease of the orientationally averaged excluded volume with number density. It follows that the densest packing density cannot be greater than the inverse of the smallest average excluded volume of a pair of particles. The orientational distribution function is therefore expected to depend sensitively on the number density ρ_0 .

To capture accurately the phase behavior, we keep the full logarithmic dependence in this work; this is the salient feature of our approach. This form of the free energy is the origin of a remarkable phenomenon: above a critical value of ρ_0 , the equilibrium distribution function $f(\hat{\mathbf{I}})$ is zero on a region of the orientation space with positive measure; that is, at high densities, some regions of orientation space are not accessible to particles.

Excluded volume: As an example, we consider a system of hard ellipsoids and provide an explicit expression for the excluded volume. For identical hard ellipsoids of revolution with length L , width W and volume v_0 , a simple approximation for the excluded volume is

$$V_{exc}(\hat{\mathbf{I}}_1, \hat{\mathbf{I}}_2) = c - \frac{2d}{3} (\sigma(\hat{\mathbf{I}}_1) : \sigma(\hat{\mathbf{I}}_2)), \quad (26)$$

$$c = v_0 \frac{4}{3} \left(\frac{L}{W} + \frac{W}{L} + 4 \right), \quad (27)$$

$$d = v_0 \frac{4}{3} \left(\frac{L}{W} + \frac{W}{L} - 2 \right). \quad (28)$$

where $\sigma(\hat{\mathbf{I}}) = \frac{1}{2}(3\hat{\mathbf{I}}\hat{\mathbf{I}} - \mathbf{I})$ denotes the orientation descriptor of a particle with symmetry axis oriented along $\hat{\mathbf{I}}$, with the shape parameters $d \geq 0$ and $c > d$. Substitution of the expression in Eq. (26-28) for the excluded volume into Eq. (24) gives for the free energy density (per unit volume),

$$\mathcal{F} = kT\rho_0 \left(\ln \rho_0 + \int_{\mathbb{S}^2} f(\hat{\mathbf{I}}) \ln f(\hat{\mathbf{I}}) d^2\hat{\mathbf{I}} - \int_{\mathbb{S}^2} f(\hat{\mathbf{I}}) \ln \left(1 - \rho_0 \left(c + d \frac{2}{3} \sigma(\hat{\mathbf{I}}) : \mathbf{Q} \right) \right) d^2\hat{\mathbf{I}} \right), \quad (29)$$

where

$$\mathbf{Q} = \int_{\mathbb{S}^2} \sigma(\hat{\mathbf{I}}) f(\hat{\mathbf{I}}) d^2\hat{\mathbf{I}}, \quad (30)$$

is the symmetric and traceless tensor orientational order parameter. The eigenvectors of \mathbf{Q} indicate the principal directions of average orientation, and the eigenvalues indicate the degree of order along the direction of the corresponding eigenvector. The eigenvalues range from $-1/2$ to 1 . Note $f(\hat{\mathbf{I}}) \geq 0$ is admissible if

$$1 - \rho_0 \left(c + d \frac{2}{3} \sigma(\hat{\mathbf{I}}) : \mathbf{Q} \right) > 0, \quad (31)$$

that is, if the argument of the logarithm is positive.

Parametrization: It is convenient to introduce the dimensionless parameter

$$\phi = \frac{\rho_0 c - 1}{\rho_0 d} \in (-\infty, 1], \quad (32)$$

which is an increasing function of number density $\rho_0 = \frac{1}{c-d\phi}$. In the very dilute limit, $\rho_0 \rightarrow 0^+$, $\phi \rightarrow -\infty$; in the dense packing limit, $\rho_0 \rightarrow \frac{1}{c-d}^-$, $\phi \rightarrow 1^-$, this corresponds to the densest packing fraction with only pairwise interactions. In terms of ϕ , the free energy density becomes, retaining the only relevant terms,

$$\mathcal{F} = kT\rho_0 \int_{\mathbb{S}^2} \left[f(\hat{\mathbf{I}}) \ln f(\hat{\mathbf{I}}) - f(\hat{\mathbf{I}}) \ln \left(\frac{2}{3} \sigma(\hat{\mathbf{I}}) : \mathbf{Q} - \phi \right) \right] d^2\hat{\mathbf{I}}. \quad (33)$$

Minimization of the free energy: We next minimize the free energy density with respect to the orientational distribution function $f(\hat{\mathbf{I}})$. We write \mathcal{F} explicitly in terms of the distribution

$$\mathcal{F} = kT\rho_0 \int_{\mathbb{S}^2} \left[f(\hat{\mathbf{I}}_1) \ln f(\hat{\mathbf{I}}_1) - f(\hat{\mathbf{I}}_1) \ln \left(\frac{2}{3} \sigma(\hat{\mathbf{I}}_1) : \int_{\mathbb{S}^2} \sigma(\hat{\mathbf{I}}_2) f(\hat{\mathbf{I}}_2) d^2 \hat{\mathbf{I}}_2 - \phi \right) \right] d^2 \hat{\mathbf{I}}_1, \quad (34)$$

where we have labelled the arguments for the sake of clarity. We have two constraints: the distribution function is normalized to unity, that is,

$$\int_{\mathbb{S}^2} f(\hat{\mathbf{I}}) d^2 \hat{\mathbf{I}} = 1, \quad (35)$$

and the argument of the logarithm, the free volume fraction, must be positive; that is

$$\frac{2}{3} \sigma(\hat{\mathbf{I}}) : \mathbf{Q} - \phi > 0. \quad (36)$$

Setting the first variation to zero gives

$$\ln f(\hat{\mathbf{I}}_1) + (\lambda + 1) - \ln \left(\frac{2}{3} \sigma(\hat{\mathbf{I}}_1) : \int_{\mathbb{S}^2} \sigma(\hat{\mathbf{I}}_2) f(\hat{\mathbf{I}}_2) d^2 \hat{\mathbf{I}}_2 - \phi \right) - \sigma(\hat{\mathbf{I}}_1) : \left(\int_{\mathbb{S}^2} f(\hat{\mathbf{I}}_2) \frac{\frac{2}{3} \sigma(\hat{\mathbf{I}}_2)}{\frac{2}{3} \sigma(\hat{\mathbf{I}}_2) : \int_{\mathbb{S}^2} \sigma(\hat{\mathbf{I}}_3) f(\hat{\mathbf{I}}_3) d^2 \hat{\mathbf{I}}_3 - \phi} d^2 \hat{\mathbf{I}}_2 \right) = 0, \quad (37)$$

where λ is a Lagrange multiplier associated with the normalization of $f(\hat{\mathbf{I}})$.

Solving for the distribution function gives the self-consistent equation for f

$$f(\hat{\mathbf{I}}_1) = \begin{cases} \frac{\int_{\mathbb{S}^2} \sigma(\hat{\mathbf{I}}_2) f(\hat{\mathbf{I}}_2) d^2 \hat{\mathbf{I}}_2 e^{\frac{\sigma(\hat{\mathbf{I}}_1) : \int_{\mathbb{S}^2} f(\hat{\mathbf{I}}_2) \frac{\frac{2}{3} \sigma(\hat{\mathbf{I}}_2)}{\frac{2}{3} \sigma(\hat{\mathbf{I}}_2) : \int_{\mathbb{S}^2} \sigma(\hat{\mathbf{I}}_3) f(\hat{\mathbf{I}}_3) d^2 \hat{\mathbf{I}}_3 - \phi} d^2 \hat{\mathbf{I}}_2}}{\int_{\mathbb{S}^2} \left(\frac{2}{3} \sigma(\hat{\mathbf{I}}_1) : \int_{\mathbb{S}^2} \sigma(\hat{\mathbf{I}}_2) f(\hat{\mathbf{I}}_2) d^2 \hat{\mathbf{I}}_2 - \phi \right) e^{\frac{\sigma(\hat{\mathbf{I}}_1) : \int_{\mathbb{S}^2} f(\hat{\mathbf{I}}_2) \frac{\frac{2}{3} \sigma(\hat{\mathbf{I}}_2)}{\frac{2}{3} \sigma(\hat{\mathbf{I}}_2) : \int_{\mathbb{S}^2} \sigma(\hat{\mathbf{I}}_3) f(\hat{\mathbf{I}}_3) d^2 \hat{\mathbf{I}}_3 - \phi} d^2 \hat{\mathbf{I}}_2}} d^2 \hat{\mathbf{I}}_1} & \text{if } \frac{2}{3} \sigma(\hat{\mathbf{I}}) : \mathbf{Q} - \phi > 0, \\ 0 & \text{o.w.} \end{cases} \quad (38)$$

or in terms of the order parameter \mathbf{Q}

$$f(\hat{\mathbf{I}}) = \begin{cases} \frac{\int_{\mathbb{S}^2} \sigma(\hat{\mathbf{I}}_2) f(\hat{\mathbf{I}}_2) \frac{\frac{2}{3} \sigma(\hat{\mathbf{I}}_2)}{\frac{2}{3} \sigma(\hat{\mathbf{I}}_2) : \mathbf{Q} - \phi} d^2 \hat{\mathbf{I}}_2 e^{\frac{\sigma(\hat{\mathbf{I}}) : \int_{\mathbb{S}^2} f(\hat{\mathbf{I}}_2) \frac{\frac{2}{3} \sigma(\hat{\mathbf{I}}_2)}{\frac{2}{3} \sigma(\hat{\mathbf{I}}_2) : \mathbf{Q} - \phi} d^2 \hat{\mathbf{I}}_2}}{\int_{\mathbb{S}^2} \left(\frac{2}{3} \sigma(\hat{\mathbf{I}}) : \mathbf{Q} - \phi \right) e^{\frac{\sigma(\hat{\mathbf{I}}) : \int_{\mathbb{S}^2} f(\hat{\mathbf{I}}_2) \frac{\frac{2}{3} \sigma(\hat{\mathbf{I}}_2)}{\frac{2}{3} \sigma(\hat{\mathbf{I}}_2) : \mathbf{Q} - \phi} d^2 \hat{\mathbf{I}}_2}} d^2 \hat{\mathbf{I}}_1} & \text{if } \frac{2}{3} \sigma(\hat{\mathbf{I}}) : \mathbf{Q} - \phi > 0, \\ 0 & \text{o.w.} \end{cases} \quad (39)$$

We define the auxiliary tensor order parameter Ψ such that

$$\Psi = \int_{\mathbb{S}^2} f(\hat{\mathbf{I}}) \frac{\frac{2}{3} \sigma(\hat{\mathbf{I}})}{\frac{2}{3} \sigma(\hat{\mathbf{I}}) : \mathbf{Q} - \phi} d^2 \hat{\mathbf{I}}. \quad (40)$$

Finally, the equation for the distribution becomes

$$f(\hat{\mathbf{I}}) = \frac{\left(\frac{2}{3} \sigma(\hat{\mathbf{I}}) : \mathbf{Q} - \phi \right) e^{\sigma(\hat{\mathbf{I}}) : \Psi}}{\int_{\mathbb{S}^2} \left(\frac{2}{3} \sigma(\hat{\mathbf{I}}) : \mathbf{Q} - \phi \right) e^{\sigma(\hat{\mathbf{I}}) : \Psi} d^2 \hat{\mathbf{I}}}, \quad (41)$$

where

$$\mathbf{Q} = \left\langle \sigma(\hat{\mathbf{I}}) \right\rangle, \quad (42)$$

and

$$\Psi = \left\langle \frac{\frac{2}{3}\sigma(\hat{\mathbf{1}})}{\frac{2}{3}\sigma(\hat{\mathbf{1}}) : \mathbf{Q} - \phi} \right\rangle. \quad (43)$$

The requirement of positivity of the free volume fraction $\frac{2}{3}\sigma(\hat{\mathbf{1}}) : \mathbf{Q} - \phi > 0$ results in the orientational distribution function being zero in some regions of orientation space. There are technical issues surrounding the validity of using the Euler-Lagrange equation to find minimisers of singular functionals like ours, but these have been addressed in [11], rigorously providing results fully consistent with our analysis.

The equation of state: To derive the equation of state of our system of hard ellipsoids, we start with the relation between the pressure and the free energy density,

$$P = -\mathcal{F} + \rho_0 \frac{\partial \mathcal{F}}{\partial \rho_0}. \quad (44)$$

Writing out all the terms

$$\mathcal{F} = kT\rho_0 \left(\ln \rho_0 + \int_{\mathbb{S}^2} f(\hat{\mathbf{1}}) \ln f(\hat{\mathbf{1}}) d^2\hat{\mathbf{1}} - \int_{\mathbb{S}^2} f(\hat{\mathbf{1}}) \ln \left(1 - \rho_0 c + \rho_0 d \frac{2}{3} \mathbf{Q} : \sigma(\hat{\mathbf{1}}) \right) d^2\hat{\mathbf{1}} \right), \quad (45)$$

and recalling Eq. (32) we get

$$\mathcal{F} = \rho_0 kT \left(-\ln d + \int_{\mathbb{S}^2} f(\hat{\mathbf{1}}) \ln f(\hat{\mathbf{1}}) d^2\hat{\mathbf{1}} - \int_{\mathbb{S}^2} f(\hat{\mathbf{1}}) \ln \left(\frac{2}{3} \mathbf{Q} : \sigma(\hat{\mathbf{1}}) - \phi \right) d^2\hat{\mathbf{1}} \right), \quad (46)$$

$$\frac{\partial \mathcal{F}}{\partial \rho_0} = \rho_0 kT \left(\int_{\mathbb{S}^2} \frac{f(\hat{\mathbf{1}})}{\frac{2}{3} \mathbf{Q} : \sigma(\hat{\mathbf{1}}) - \phi} d\hat{\mathbf{1}} \right) \frac{\partial \phi}{\partial \rho_0} + kT \left[-\ln d + \int_{\mathbb{S}^2} f(\hat{\mathbf{1}}) \ln f(\hat{\mathbf{1}}) d^2\hat{\mathbf{1}} - \int_{\mathbb{S}^2} f(\hat{\mathbf{1}}) \ln \left(\frac{2}{3} \mathbf{Q} : \sigma(\hat{\mathbf{1}}) - \phi \right) d^2\hat{\mathbf{1}} \right] \quad (47)$$

$$\frac{\partial \phi}{\partial \rho_0} = \frac{1}{d\rho_0^2}, \rho_0 \frac{\partial \phi}{\partial \rho_0} = \frac{1}{\rho_0 d}, \quad (48)$$

$$P = \rho_0 kT \left(\frac{1}{\rho_0 d} \int_{\mathbb{S}^2} \frac{f}{\frac{2}{3} \mathbf{Q} : \sigma(\hat{\mathbf{1}}) - \phi} d\hat{\mathbf{1}} \right) = kT \frac{1}{d} \left\langle \frac{1}{\frac{2}{3} \mathbf{Q} : \sigma(\hat{\mathbf{1}}) - \phi} \right\rangle. \quad (49)$$

or

$$P = \frac{\rho_0 kT}{1 - \rho_0 c} \left\langle \frac{\phi}{\phi - \frac{2}{3} \mathbf{Q} : \sigma(\hat{\mathbf{1}})} \right\rangle. \quad (50)$$

If $\mathbf{Q} = 0$, then we have

$$P = \frac{\rho_0 kT}{1 - \rho_0 c} \quad (51)$$

as in the Van der Waals case without attractive interactions. In general, Eq. (50) is our equation of state. We shall show numerically that in high density regime, when ϕ approaches 1, the pressure approaches infinity.

3 The assumption of uniaxiality

Without external fields, classical models (Maier-Saupe model [12] for attractive interactions, Onsager model [1] for steric interactions), predict only uniaxial nematic order at high densities [13]. In this section, we shall assume that \mathbf{Q} is uniaxial to simplify the presentation. Below, we will

demonstrate that biaxial equilibrium \mathbf{Q} also exists, but only as an unstable saddle point, thus not observable physically. Under the uniaxiality assumption, \mathbf{Q} can be represented as

$$\mathbf{Q} = \frac{S}{2}(3\hat{\mathbf{n}}\hat{\mathbf{n}} - \mathbf{I}), \quad (52)$$

where S is the scalar order parameter, indicating the degree of order, and $\hat{\mathbf{n}}$ is the nematic director, a unit vector indicating direction of average orientation. One can show that Ψ is also uniaxial, and shares the same eigenframe with \mathbf{Q} , thus can be written as

$$\Psi = \Psi(\hat{\mathbf{n}}\hat{\mathbf{n}} - \frac{1}{3}\mathbf{I}). \quad (53)$$

The uniaxiality assumption makes the analysis and numerics more tractable. Now

$$\begin{aligned} \mathbf{Q} : \sigma(\hat{\mathbf{I}}) &= \frac{3S}{2}P_2(\hat{\mathbf{n}} \cdot \hat{\mathbf{I}}), \\ \Psi : \sigma(\hat{\mathbf{I}}) &= \Psi P_2(\hat{\mathbf{n}} \cdot \hat{\mathbf{I}}), \end{aligned} \quad (54)$$

where $P_2(x)$ is the second order Legendre polynomial, and the free energy density becomes

$$\mathcal{F} = \rho_0 kT \left(\int_{\mathbb{S}^2} f(\hat{\mathbf{I}}) \ln f(\hat{\mathbf{I}}) d^2\hat{\mathbf{I}} - \int_{\mathbb{S}^2} f(\hat{\mathbf{I}}) \ln(SP_2(\hat{\mathbf{n}} \cdot \hat{\mathbf{I}}) - \phi) d^2\hat{\mathbf{I}} \right) \quad (55)$$

$$= 2\pi\rho_0 kT \left(\Psi S - \ln \int_{\mathbb{S}_+^2} (SP_2(x) - \phi) e^{\Psi P_2(x)} dx \right), \quad (56)$$

where $x = \hat{\mathbf{n}} \cdot \hat{\mathbf{I}} = \cos \theta$, and $\mathbb{S}_+^2 = \{x : SP_2(x) - \phi > 0\}$. The distribution function is now given by

$$f(x) = \begin{cases} \frac{(SP_2(x) - \phi) \exp(\Psi P_2(x))}{\int_{\mathbb{S}_+^2} (SP_2(x) - \phi) \exp(\Psi P_2(x)) dx} & \text{if } SP_2(x) - \phi > 0 \\ 0 & \text{o.w.} \end{cases} \quad (57)$$

Instead of solving the above self-consistent equation for $f(x)$, we solve the coupled equations for Ψ and S ,

$$S = \frac{\int_{\mathbb{S}_+^2} P_2(x) (SP_2(x) - \phi) \exp(\Psi P_2(x)) dx}{\int_{\mathbb{S}_+^2} (SP_2(x) - \phi) \exp(\Psi P_2(x)) dx} = \langle P_2(x) \rangle, \quad (58)$$

$$\Psi = \frac{\int_{\mathbb{S}_+^2} P_2(x) \exp(\Psi P_2(x)) dx}{\int_{\mathbb{S}_+^2} (SP_2(x) - \phi) \exp(\Psi P_2(x)) dx} = \left\langle \frac{P_2(x)}{SP_2(x) - \phi} \right\rangle. \quad (59)$$

The integration limits, explicitly, are

$$(x_0, 1), \text{ if } S > 0, \quad (60)$$

$$(0, x_0), \text{ if } S < 0. \quad (61)$$

and $x_0 > 0$ is such that $P_2(x_0) = \phi/S$.⁴ To solve the above equations efficiently, we convert them to the following self-consistent equation for the integration limits x_0 ,

$$\frac{1}{\Psi} + P_2(x_0) = \frac{\int_{x_0}^1 P_2^2(x) \exp(\Psi P_2(x)) dx}{\int_{x_0}^1 P_2(x) \exp(\Psi P_2(x)) dx}, \text{ if } S > 0, \quad (62)$$

$$\frac{1}{\Psi} + P_2(x_0) = \frac{\int_0^{x_0} P_2^2(x) \exp(\Psi P_2(x)) dx}{\int_0^{x_0} P_2(x) \exp(\Psi P_2(x)) dx}, \text{ if } S < 0. \quad (63)$$

⁴We study f only for $0 \leq x \leq 1$, as it is clearly even in $-1 \leq x \leq 1$.

These two equations are solved separately. For each of them, we first assign a value for $\Psi \in (-\infty, \infty)$, then x_0 is found by using the built in root finding routine in Wolfram Mathematica. Next, since $\phi/S = P_2(x_0)$, the order parameter S can be evaluated from Eq. (58). Finally ϕ can be obtained from $\phi = SP_2(x_0)$. This way, we associate each value of Ψ with scalar order parameter S and number density parameter ϕ .

A special point. The point $\Psi = 0$ is a singular point of the above equations. In this case, we consider the Eq. (59) directly. It is easy to show that the integration limit $x_0 = 0$ if $S > 0$, $x_0 = 1$ if $S < 0$. By setting $\Psi = 0$ in Eq. (58), we get $\phi = -0.2$. To satisfy the constraint

$$SP_2(x_0) > \phi, \quad (64)$$

we immediately arrive at the following range for S ,

$$-0.2 < S < 0.4. \quad (65)$$

That is, for $\Psi = 0$, corresponding to $\phi = -0.2$, any value of $S \in (-0.2, 0.4)$ is a solution of EL equation.

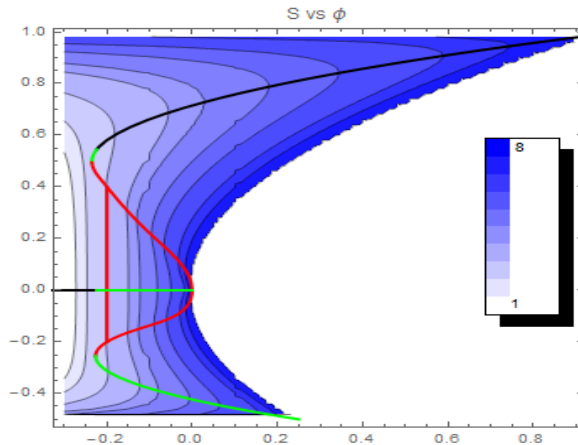


Figure 1: Equilibrium order parameter S vs. ϕ with uniaxial solutions only, superimposed by energy density contours. The black curve represents the stable branch of the bifurcation, the green curves correspond to the metastable branch, and the red curves to the unstable branch.

Fig. 1 is our key result. It shows the equilibrium uniaxial order parameter S vs. ϕ . The stabilities of different branches are determined by examining the convexity of the free energy density surface. To effectively illustrate this, the contours of free energy density are superimposed on the bifurcation graph in the $S-\phi$ plane. The black curve represents the stable branch. The green curves correspond to metastable states, and the red curves indicate unstable regimes. For $\phi < \phi_{NI} = -0.224$, the system is in the isotropic state with $S = 0$; at $\phi = \phi_{NI}$, the system undergoes a first order transition to nematic state, with order parameter $S_{NI} = 0.545$. As $\phi \rightarrow 1$, the order parameter $S \rightarrow 1$ indicating a completely aligned configuration. Inside the blue parabola are the regions where the ordered state/order parameters are not admissible. At $\phi = -0.2$, the vertical red line indicates that all values of $-0.2 < S < 0.4$ share the same energy.

In Fig. 2, representative orientational probability density functions are presented as a density plot on the surface of a unit sphere for different equilibrium uniaxial solutions shown on Fig. 1. In those graphs, the z -axis is chosen to be along the uniaxial director, thus the density plots are axi-symmetric with respect to the z -axis. The density functions are continuous, and normalized

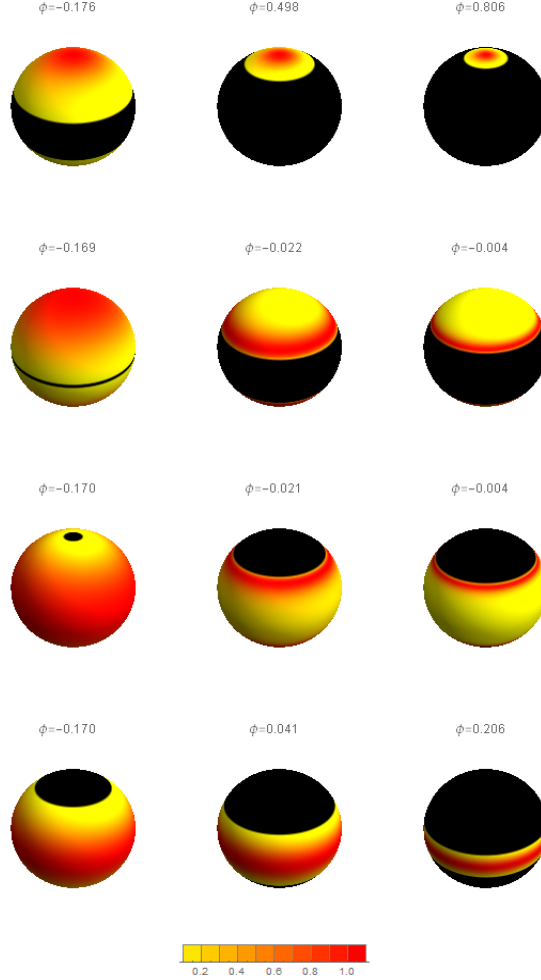


Figure 2: Density plot of the orientational distribution function for selected equilibrium uniaxial solutions. Top row: stable configuration with order parameter $S > 0$; Second row: metastable configuration with $S > 0$; Third row: Unstable saddle point configuration with $S < 0$; Bottom row: metastable configuration with $S < 0$.

by their maximum values on each sphere. The black regions on the spheres indicate forbidden orientations, i.e., no particles are allowed to orient in directions corresponding to those regions. Yellow indicates only a few particles oriented in that direction, and red indicates that the majority of particles are oriented in that direction. The figures clearly reveal that the allowed regions of orientation shrink as the number density increases. This effect is further illustrated in Fig. 3.

Fig. 3 shows the lower (upper) limit x_0 of the integration for $S > 0$ ($S < 0$). The pdf has no forbidden region when $\Psi = 0$. As one traces the stable black branch in the direction of increasing ϕ , the region shrinks. As $\phi \rightarrow 1$, the upper limit $x_0 \rightarrow 1$, which implies that all particles orient precisely in the same direction, that is, they are perfectly ordered. At the lowest green branch, as $\phi \rightarrow 1/4$, the lower limit $x_0 \rightarrow 0$, the particles all lie in the plane perpendicular to the unique direction (normal to the plane), but are randomly oriented in the plane. On the unstable red branches, the particles are oriented inside or outside a cone, but more towards the boundary of that cone, as shown in the second and third row in Fig. 2.

Fig. 4 shows the pressure vs. ϕ for all uniaxial equilibrium solutions. Clearly, the pressure

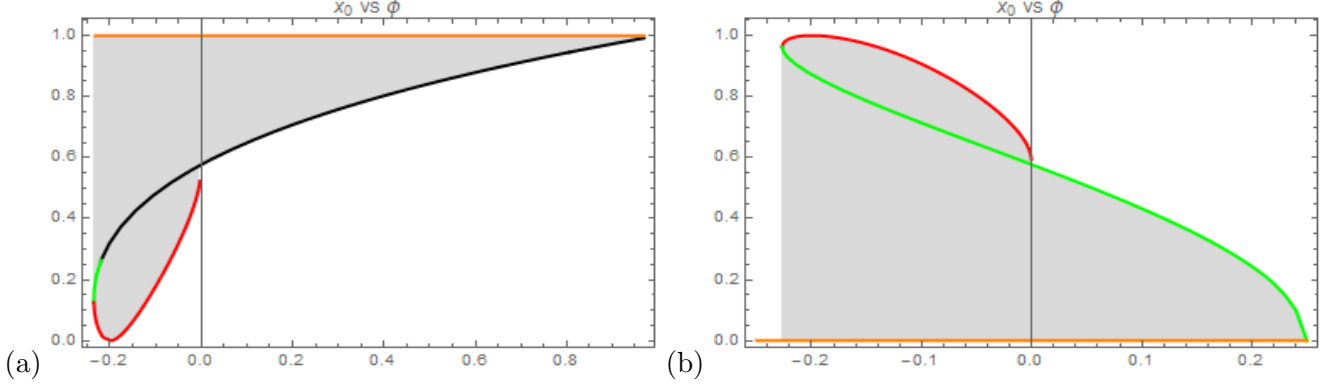


Figure 3: (a) Lower integration limit x_0 vs. ϕ for uniaxial equilibrium solutions with $S > 0$; and the top horizontal line indicates the upper limit of the integration. (b) Upper limit x_0 vs. ϕ for equilibrium solutions with $S < 0$; and the bottom horizontal line indicates the lower limit of the integration. Black, green and red colors correspond to stable, metastable, and unstable solutions in Fig. 1.

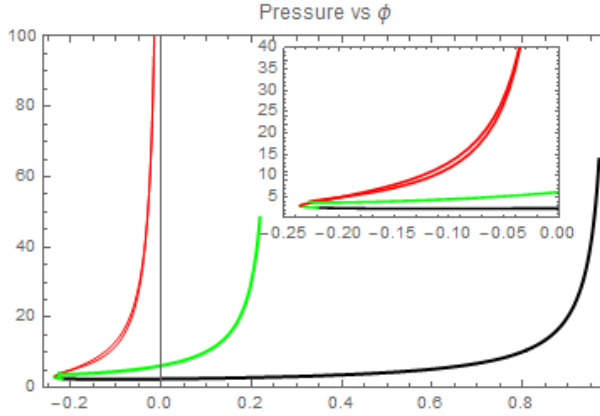


Figure 4: Pressure vs. ϕ for uniaxial equilibrium solutions.

increases nonlinearly as the number density increases, and diverges at a certain finite number density. It is interesting to note that the pressures for the red and green branches are much greater than for the black branch.

4 Biaxial equilibrium solutions

We suspect the existence of biaxial equilibrium solutions, especially for $\phi > 0$, since the energy graph for each $\phi > 0$ corresponds to two separated branches, with inadmissible regions in between, and energy diverges as S gets close to the boundary of the inadmissible region as seen in Fig. 1. If the system starts with a configuration with $S < 0$ near the metastable phase, it has to make its way to the lowest energy state, and the only way is through biaxial phases. In the eigenframe of \mathbf{Q} , \mathbf{Q} can be represented by

$$\mathbf{Q} = \text{diag}\left(r \cos\left(\alpha + \frac{2\pi}{3}\right), r \cos\left(\alpha - \frac{2\pi}{3}\right), r \cos \alpha\right), \quad (66)$$

thus \mathbf{Q} is fully characterized by r and α [14]. We use the ternary diagram to represent \mathbf{Q} 's. Consider an equilateral triangle with sides of unit length, centered at the origin, with one vertex on the positive y -axis. Each point in the triangle corresponds to a set of eigenvalues of \mathbf{Q} . To obtain the eigenvalues of \mathbf{Q} , we draw lines parallel to each edge, through the point. Each line intersects two edges, the length of the line segment from the point of intersection to the vertex gives the eigenvalues of $\mathbf{Q} + \mathbf{I}/3$. We illustrate this by Fig. 5. Due to symmetry, we only consider 1/6 portion of the triangle (shaded), and the rest corresponds to 5 different permutations of the same sets of eigenvalues of \mathbf{Q} . Given two coordinates (x, y) , $0 < x < \sqrt{3}/2$, $-1/2 < y < \sqrt{3}x/3$ of a point, r and α can be found by

$$r = \sqrt{(x^2 + y^2)} = \sqrt{\frac{2}{3}\mathbf{Q} : \mathbf{Q}}, \quad (67)$$

$$\alpha = -\frac{\pi}{6} - \arctan \frac{y}{x}. \quad (68)$$

Here $r = 0$, for which $\mathbf{Q} = \text{diag}(0, 0, 0)$, corresponds to the isotropic phase (the upper left corner of the shaded triangle in Fig. 5); $\alpha = 0$, for which $\mathbf{Q} = \text{diag}(-r/2, -r/2, r)$, corresponds to uniaxial prolate phases (the hypotenuse), and $\alpha = \pi/3$, for which $\mathbf{Q} = \text{diag}(-r, r/2, r/2)$, corresponds to uniaxial oblate phases (the short vertical edge); $\alpha = \pi/6$, for which $\mathbf{Q} = \text{diag}(-\sqrt{3}r/2, 0, \sqrt{3}r/2)$, correspond to biaxial phase with largest biaxiality.

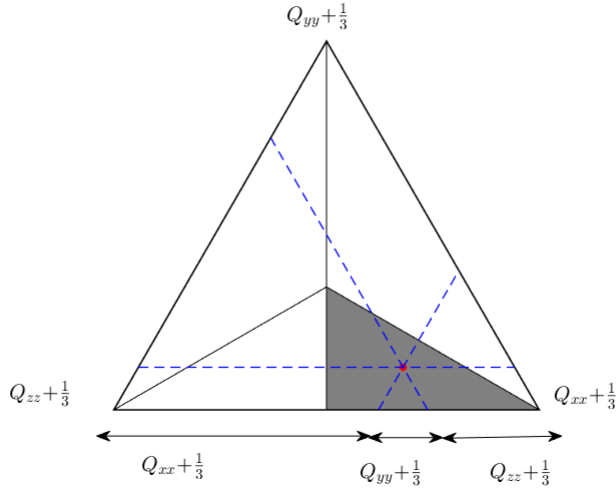


Figure 5: Ternary diagram for representing \mathbf{Q} .

We select two representative values of ϕ to examine the landscape of the free energy density vs. \mathbf{Q} . For each value of ϕ , we specify \mathbf{Q} , and numerically solve for Ψ using an iterative Newton's method, and then numerically evaluate the energy density. In Fig. 6, energy density contours are plotted vs. different \mathbf{Q} . For $\phi = -0.1$, there are six critical points on the energy surface: one isotropic local minimizer, one prolate uniaxial global minimizer, one uniaxial oblate local maximizer along the hypotenuse, one uniaxial oblate local minimizer, one uniaxial oblate saddle point along the short vertical edge, and one biaxial saddle point in the interior of the triangle. For $\phi = 0.1$, there are three critical points: one uniaxial prolate local minimizer along the hypotenuse, one uniaxial oblate local minimizer along the short vertical edge, and one biaxial saddle point in the interior of the triangle. The energy blows up when $r^2 < \phi$, so there is an inadmissible region in the upper left

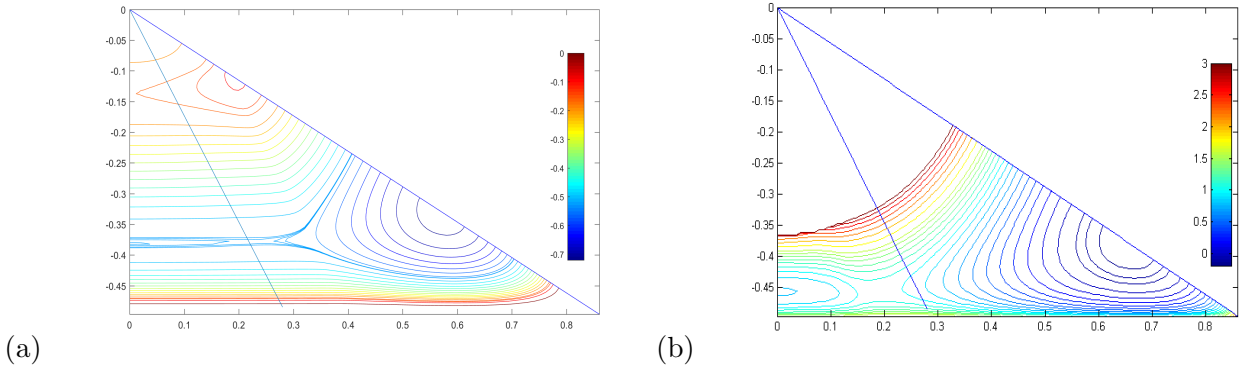


Figure 6: Energy contours for two representative volume fractions. (a) $\phi = -0.1$; (b) $\phi = 0.1$.

portion of the triangle. Thus it suggests that for any value of ϕ large enough, if $S < 0$ is one of the equilibrium uniaxial solution, there will be a saddle point biaxial equilibrium solution. This was also not reported in Onsager’s work, nor, as far as we know, in any model for uniaxial particles without an external field.

5 Conclusions

In this paper, we study a system of ellipsoidal particles interacting only via hard core interactions. We consider the canonical ensemble, and derive an expression for the free energy density. The free energy density contains a logarithmic term, which, upon expansion, is in agreement with Onsager’s model. We argue that Onsager’s model predicts the correct phase behavior near the nematic-isotropic transition, but it fails to give the correct equation of state; the pressure does not diverge as the number density is increased without limit. Thus, Onsager’s model cannot be used to accurately describe dense nematics. Our work, essential and approximate as it may be, provides a starting point toward studying dense nematic systems. The derivation of the free energy is in the mean field spirit, and the results predicted from the model might not agree quantitatively with experiment, but we hope it will show at least qualitative agreement.

With the uniaxial assumption, we were able to simplify the self-consistent equations and to demonstrate a bifurcation landscape which is much richer than that of Onsager. A striking result is that almost all equilibrium probability density functions have a forbidden region in orientation space. As the number density increases, the regions of forbidden orientations grow, and the degree of orientational order increases. Our model predicts a first order Nematic-Isotropic phase transition, and complete alignment in a dense packing limit. We have further demonstrated that a biaxial equilibrium solution exists, but only as a saddle point.

Acknowledgement 1 *X.Z. and P.P-M acknowledge support from NSF under DMS-1212046 and EFRI-1332271. J.M.T acknowledges support from European Research Council under the European Union’s Seventh Framework Programme (FP7/2007-2013) / ERC grant agreement n° 291053. E.G.V. acknowledges the kind hospitality of the Oxford centre for Nonlinear PDE, where part of this work was done while he was visiting the Mathematical Institute at the University of Oxford.*

References

- [1] Onsager, L., The effects of shape on the interaction of colloidal particles. *Annals of the New York Academy of Sciences*, **51**(4), 627-659 (1949).
- [2] Frenkel, D., and B. M. Mulder. The hard ellipsoid-of-revolution fluid: I. Monte Carlo simulations. *Molecular physics* **55** (5), 1171-1192 (1985).
- [3] Palffy-Muhoray, P., Virga, E.G., and Zheng, X., Towards Onsager's density functional via Penrose's tree indentivity, to be submitted (2017).
- [4] Sheng, P., Hard Rod Model of the Nematic-Isotropic Phase, in Introduction to Liquid Crystals, Springer, (1975).
- [5] Taylor, M.P., and Herzfeld, Nematic and smectic order in a fluid of biaxial hard particles, *J. Phys. Rev. A*, **44**, 3742 (1991).
- [6] Malijevsky, A., Jackson, G., and Varga, S., Many-fluid Onsager density functional theories for orientational ordering in mixtures of anisotropic hard-body fluids, *The Journal of Chemical Physics*, **129**, 144504 (2008).
- [7] Wu, L., Malijevsky, A., Jackson, G., Muller, E. A., and Avendano, C., Orientational ordering and phase behaviour of binary mixtures of hard spheres and hard spherocylinders, *The Journal of Chemical Physics*, **143**, 044906 (2015).
- [8] Doi, M., and Edwards, S.F., The theory of Polymer Dynamics, p. 354, (Clarendon, Oxford 1986).
- [9] van Kampen, N.G., Condensation of a classical gas with long range attraction, *Phy. Rev.*, **135**, A362 (1964).
- [10] Tonks, L., The complete equation of state of one, two and three-dimensional gases of hard elastic spheres, *Phys. Rev.*, **50**, 955 (1936).
- [11] Taylor, J. M., An analysis of equilibria in dense nematic liquid crystals, to be submitted, (2017).
- [12] Maier, W., and Saupe, A, *Z. Naturforsch A*, **13**(a), 564-566 (1958).
- [13] Fatkullin, I., and Slastikov, V. Critical points of the Onsager functional on a sphere, *Nonlinearity*, **18**, 2565-2580 (2005).
- [14] Zheng, X., and Palffy-Muhoray, P., One order parameter tensor mean field theory for biaxial liquid crystals, *Discrete and Continuous Dynamical Systems, Series B*, **15**(2), 475-490 (2011).